



Brazilian Journal of Physics  
ISSN: 0103-9733  
luizno.bjp@gmail.com  
Sociedade Brasileira de Física  
Brasil

Alam, M. S.; Masud, M. M.; Mamun, A. A.  
Ion-Scale Electrostatic Nonplanar Shock Waves in Dusty Plasmas with Two-Temperature  
Superthermal Electrons  
Brazilian Journal of Physics, vol. 45, núm. 1, 2015, pp. 95-101  
Sociedade Brasileira de Física  
São Paulo, Brasil

Available in: <http://www.redalyc.org/articulo.oa?id=46433753014>

- How to cite
- Complete issue
- More information about this article
- Journal's homepage in [redalyc.org](http://redalyc.org)

[redalyc.org](http://redalyc.org)

Scientific Information System  
Network of Scientific Journals from Latin America, the Caribbean, Spain and Portugal  
Non-profit academic project, developed under the open access initiative

# Ion-Scale Electrostatic Nonplanar Shock Waves in Dusty Plasmas with Two-Temperature Superthermal Electrons

M. S. Alam · M. M. Masud · A. A. Mamun

Received: 3 September 2014 / Published online: 5 December 2014  
© Sociedade Brasileira de Física 2014

**Abstract** The basic properties of nonplanar (viz. cylindrical and spherical) dust-ion-acoustic (DIA) shock waves in an unmagnetized dusty plasma system [consisting of inertial ions, negatively charged immobile dust, and superthermal electrons with two distinct temperatures] are investigated by employing the reductive perturbation method. The modified Burgers equation is derived and is numerically analyzed in order to examine the basic properties of DIA shock structures. The effects of nonplanar geometry, electron superthermality, and ion kinematic viscosity on the basic features of DIA shock waves are discussed. It is found that the properties of the cylindrical and spherical DIA shock waves in dusty plasmas with two-temperature superthermal electrons significantly differ from those of one-dimensional planar shocks. The implications of our results in space plasmas [viz. star formation, supernovae explosion, solar wind, pulsar magnetosphere, Saturn's outer magnetosphere ( $R \sim 13\text{--}18 R_S$ , where  $R_S$  is the radius of Saturn), Saturn's inner magnetosphere ( $R < 9 R_S$ , etc.)] and laboratory plasmas (viz. laser-induced implosion, capsule implosion, shock

tube, etc.), where superthermal electrons with two distinct temperatures occurs, are briefly discussed.

**Keywords** Nonplanar shock waves · Modified Burgers equation · Dust-ion-acoustic waves · Two-temperature electrons · Superthermal electrons · Kappa distribution

## 1 Introduction

Significant part of the studies on dusty plasmas involving theory and experiments is based on the analysis of linear and nonlinear waves in dusty plasmas. One of the most important and interesting nonlinear phenomena in plasma physics is dust-ion-acoustic (DIA) waves. About two decades ago, the existence of novel DIA waves has been shown theoretically by D'Angelo [1] and Shukla and Silin [2]. Barkan et al. [3] and Nakamura et al. [4] have observed the DIA waves by the laboratory experiments.

Nowadays, the propagation of shock waves in dusty plasmas has received considerable attention and has been extensively studied both theoretically and experimentally. Shock waves are generally formed due to the balance between nonlinearity and dissipation. Dissipation is one of the processes that play vital roles in the formation and propagation of the shock structures [5]. This dissipation arises due to the effects of the Landau damping, kinematic viscosity among the plasma species, and the collision between ion-neutral, dust-neutral, etc. The DIA shock waves have been observed by Nakamura et al. [4, 6] in a collisionally dominated dusty plasma. The nonlinear features of DIA shock waves have been investigated by many authors [4, 7–10].

Most of the studies on the DIA shock waves [4, 7–9] are based on single-temperature electrons/ions. Also, most of the investigations have been centered on Maxwellian

---

M. S. Alam (✉)  
Department of Physics,  
Jahangirnagar University,  
Savar, Dhaka, 1342, Bangladesh  
e-mail: soyonplasma@gmail.com

M. M. Masud  
Department of Physics,  
Bangladesh University of Engineering and Technology,  
Dhaka, Bangladesh

A. A. Mamun  
Jahangirnagar University,  
Savar, Dhaka 1342, Bangladesh

plasmas. Some authors have also studied non-Maxwellian plasmas with only one electron component, for instance, in the form of the Cairns distribution, Tsallis distribution, and kappa distribution [10–13].

Maxwellian distribution may be deficient for describing the long-range interactions in unmagnetized collisionless plasma where the nonequilibrium stationary state exists. However, a lot of theoretical observations of space plasmas [13, 14] are often characterized by a particle distribution function with high-energy tail and they may deviate from the Maxwellian. Superthermal particles may arise due to the effect of external forces acting on the natural space environment plasmas or to wave particle interaction. Plasmas with an excess of superthermal non-Maxwellian electrons are generally characterized by a long tail in the high-energy region. Such space plasmas can be modeled by generalized Lorentzian or kappa distribution [13, 15–18] rather than the Maxwellian distribution.

The isotropic (3D) kappa distribution function takes the form [15, 19–21]:

$$F_{\kappa}(v) = \frac{\Gamma(\kappa + 1)}{(\pi\kappa\theta^2)^{3/2}\Gamma(\kappa - 1/2)} \left(1 + \frac{v^2}{\kappa\theta^2}\right)^{-(\kappa+1)},$$

where  $\theta$  is the most probable speed (effective thermal speed) related to the usual thermal velocity  $V_t = (k_B T/m)^{1/2}$  by  $\theta = [(2\kappa - 3)/\kappa]^{1/2} V_t$ ,  $T$  being the characteristic kinetic temperature, i.e., the temperature of the equivalent Maxwellian with the same average kinetic energy [18], and  $k_B$  is the Boltzmann constant. The  $\kappa$  distribution is defined for  $\kappa > 3/2$ . The parameter  $\kappa$  is the spectral index, which is a measure of the slope of the energy spectrum of the superthermal particles forming the tail of the velocity distribution function. In the limit  $\kappa \rightarrow \infty$ , the above kappa distribution function for electrons reduces to the well-known Maxwell-Boltzmann distribution.

Sultana et al. [10] investigated the propagation of planar ion-acoustic (IA) shocks in an unmagnetized collisionless electron-ion plasma consisting of superthermal electrons and cold viscous ions. Alinejad et al. [22] analyzed the nonlinear propagation of DIA shock waves in a charge-varying dusty plasma with electrons having kappa velocity distribution. Shahmansouri and Alinejad [23] studied the dust acoustic (DA) shock waves in a charge-varying dusty plasma with ions and electrons having kappa velocity distribution. They observed that dust charge fluctuation and electrons/ions superthermality effects significantly modify the basic properties of DA shock waves. Alam et al. [24] studied the planar DIA shock waves in an unmagnetized plasma with bi-kappa distributed electrons. The plasmas composed of two-temperature superthermal (kappa-distributed)

electrons [20, 25–32] are very relevant to the Saturnian magnetosphere [26, 27, 30].

However, most of the theoretical works on the DIA or DA shock waves [4, 7–10, 22–24] are based on one-dimensional (1D) unbounded planar geometry which may not be a realistic situation for laboratory devices. The non-planar geometries of practical interest are capsule implosion (spherical geometry), shock tube (cylindrical geometry), star formation, supernova explosions, etc. [33].

Xue [34] investigated the effects of the bounded non-planar geometry on DIA shock waves in an unmagnetized dusty plasma system consisting of warm inertial ions, single-temperature Boltzmann-distributed electrons, and negatively charged immobile dust particles. Mamun and Shukla [35] also investigated the cylindrical and spherical DIA shock waves in an unmagnetized dusty plasma with single-temperature Boltzmann-distributed electrons. Recently, Sahu and Tribeche [36] studied the nonplanar electron-acoustic shock waves in an unmagnetized plasma consisting of cold electrons, immobile ions, and hot electrons featuring Tsallis distribution. Yasmin et al. [37] investigated the propagation of DIA shock waves in an unmagnetized plasma system consisting of inertial ions, non-extensive q-distributed electrons, and negatively charged immobile dust in bounded non-planar geometry. Ghosh et al. [38] have investigated the nonplanar shock structures of IA waves considering single-temperature superthermal electrons. However, the presence of dust as well as two-temperature electrons were not considered there.

The above theoretical investigations [34–36, 38] show that the properties of shock waves in bounded nonplanar (cylindrical and spherical) geometry are very discrepant from those in unbounded planar geometry. To the best of our knowledge, no theoretical investigation has been performed in considering the nonplanar geometries (cylindrical and spherical geometries) for the DIA shock structures in dusty plasmas comprising of inertial ions, negatively charged static dust, and two-temperature superthermal (kappa distributed) electrons.

In this paper, we present an investigation of the nature and characteristics of cylindrical and spherical DIA shock waves in those plasma environments along with the effects of double kappa electrons which is very relevant to the Saturnian magnetosphere [26, 30]. This is why, we consider ion continuity and momentum equations, supplemented by the kappa electron density distributions with two temperatures, to derive the modified Burgers equation.

The manuscript is organized as follows: The basic equations are presented in Section 2. The modified Burgers (MB) equation is derived in Section 3. The basic features of the shock waves are numerically analyzed and discussed in Section 4. Finally, a brief discussion is provided in Section 5.

### 2 Governing Equations

We consider an unmagnetized dusty plasma, whose constituents are inertial ions, negatively charged immobile dust, and superthermal (kappa distributed) electrons with two distinct temperatures. The nonlinear dynamics of the nonplanar DIA shock waves, whose phase speed is much smaller than electron thermal speed but larger than ion thermal speed, is governed by

$$\frac{\partial n_i}{\partial t} + \frac{1}{r^\nu} \frac{\partial}{\partial r} (r^\nu n_i u_i) = 0, \tag{1}$$

$$\frac{\partial u_i}{\partial t} + u_i \frac{\partial u_i}{\partial r} = -\frac{\partial \phi}{\partial r} + \eta \frac{1}{r^\nu} \frac{\partial}{\partial r} (r^\nu \frac{\partial u_i}{\partial r}), \tag{2}$$

$$\frac{1}{r^\nu} \frac{\partial}{\partial r} \left( r^\nu \frac{\partial \phi}{\partial r} \right) = \mu + \mu_{e1} \left( 1 - \frac{\sigma_1 \phi}{\kappa_{e1} - \frac{3}{2}} \right)^{-\kappa_{e1} + \frac{1}{2}} + \mu_{e2} \left( 1 - \frac{\sigma_2 \phi}{\kappa_{e2} - \frac{3}{2}} \right)^{-\kappa_{e2} + \frac{1}{2}} - n_i, \tag{3}$$

where  $\nu = 0$  for 1D planar geometry,  $\nu = 1$  (2) for a nonplanar cylindrical (spherical) geometry,  $n_i$  is the ion particle number density normalized by its equilibrium value  $n_{i0}$ ,  $u_i$  is the ion fluid speed normalized by  $C_i = (k_B T_{ef}/m_i)^{1/2}$ ,  $\eta$  is the viscosity coefficient normalized by  $m_i n_{i0} \omega_{pi} \lambda_{Dm}^2$ , and  $\phi$  is the electrostatic wave potential normalized by  $k_B T_{ef}/e$ ,  $\sigma_1 = T_{ef}/T_{e1}$ ,  $\sigma_2 = T_{ef}/T_{e2}$ ,  $\mu_{e1} = n_{e10}/n_{i0}$ ,  $\mu_{e2} = n_{e20}/n_{i0}$ ,  $\mu = Z_d n_{d0}/n_{i0} = 1 - \mu_{e1} - \mu_{e2}$  where  $T_{ef} = n_{e0} T_{e1} T_{e2} / (n_{e10} T_{e2} + n_{e20} T_{e1})$ . Here,  $n_{e0}$  is the total electron number density at equilibrium. It should be noted that  $T_{e1}$  ( $T_{e2}$ ) is the lower (higher) electron temperature,  $T_{ef}$  is the effective temperature of two electrons,  $T_i$  is the ion temperature,  $k_B$  is the Boltzmann constant, and  $e$  is the magnitude of the electron charge. The time variable  $t$  is normalized by  $\omega_{pi}^{-1} = (m_i/4\pi n_{i0} e^2)^{1/2}$  and the radial space variable  $r$  is normalized by  $\lambda_{Dm} = (k_B T_{ef}/4\pi n_{i0} e^2)^{1/2}$ .

### 3 Derivation of MB Equation

To investigate ingoing solutions of (1)–(3), we introduce the stretched coordinates [39]:

$$\xi = \epsilon(r - V_p t), \tag{4}$$

$$\tau = \epsilon^2 t, \tag{5}$$

where  $\epsilon$  is expansion parameter ( $0 < \epsilon < 1$ ) which fixes up the suitable scaling of the physical quantities [39]. We note that we choose the scaling of the physical quantities by introducing  $\epsilon$  in such a way that the dispersion term [the left hand side of (3)] can be omitted, but the dissipative term [the second term in right hand side of (2)] can be taken into account. However, this assumption is valid for long wavelength DIA waves which exist in many space and laboratory dusty plasma situations [1–4, 40].

Here,  $V_p$  (normalized by  $C_i$ ) is the phase speed ( $\omega/k$ ) of the perturbation mode. The variables  $n_i$ ,  $u_i$ , and  $\phi$  can be expanded in power series of  $\epsilon$ . Let  $S$  be any of the system variables  $n_i$ ,  $u_i$ , and  $\phi$ , describing the systems’s state at a given position and instant. We consider small deviations from the equilibrium state  $S^{(0)}$ , which explicitly is  $n_i^{(0)} = 1$ ,  $u_i^{(0)} = 0$ , and  $\phi^{(0)} = 0$  by taking

$$S = S^{(0)} + \sum_{n=1}^{\infty} \epsilon^n S^{(n)}. \tag{6}$$

Now, expressing (1)–(3) in terms of  $\xi$  and  $\tau$  and substituting (6) into the resulting equations, one can easily develop different sets of equations in various powers of  $\epsilon$ . To the lowest order in  $\epsilon$ , one obtains

$$u_i^{(1)} = \frac{1}{V_p} \psi, \tag{7}$$

$$n_i^{(1)} = \frac{1}{V_p^2} \psi, \tag{8}$$

$$\frac{1}{V_p^2} = \frac{\mu_{e1} (\kappa_{e1} - \frac{1}{2}) \sigma_1}{\kappa_{e1} - \frac{3}{2}} + \frac{\mu_{e2} (\kappa_{e2} - \frac{1}{2}) \sigma_2}{\kappa_{e2} - \frac{3}{2}}, \tag{9}$$

where  $\psi = \phi^{(1)}$ . Equation 9 describes the phase speed of the DIA waves propagating in a dusty plasma system under consideration where population of two-temperature superthermal electrons significantly modify the basic features of the phase speed of the DIA wave. To the next higher order in  $\epsilon$ , we obtain a set of equations, which, after using (7)–(9), can be simplified as

$$\frac{\partial n_i^{(1)}}{\partial \tau} - V_p \frac{\partial n_i^{(2)}}{\partial \xi} + \frac{\partial u_i^{(2)}}{\partial \xi} + \frac{\partial}{\partial \xi} \left[ n_i^{(1)} u_i^{(1)} \right] + \frac{u_i^{(1)} \nu}{V_p \tau} = 0, \tag{10}$$

$$\frac{\partial u_i^{(1)}}{\partial \tau} - V_p \frac{\partial u_i^{(2)}}{\partial \xi} + u_i^{(1)} \frac{\partial u_i^{(1)}}{\partial \xi} + \frac{\partial \phi^{(2)}}{\partial \xi} - \eta \frac{\partial^2 u_i^{(1)}}{\partial \xi^2} = 0, \tag{11}$$

$$\frac{\mu_{e1} P_1 P_2 \sigma_1^2}{P_3^2} \psi \frac{\partial \psi}{\partial \xi} + \frac{\partial n_i^{(2)}}{\partial \xi} + \frac{\mu_{e2} P_4 P_5 \sigma_2^2}{P_6^2} \psi \frac{\partial \psi}{\partial \xi} - \frac{\mu_{e1} P_1 \sigma_1}{P_3} \frac{\partial \phi^{(2)}}{\partial \xi} + \frac{\mu_{e2} P_4 \sigma_2}{P_6} \frac{\partial \phi^{(2)}}{\partial \xi} = 0, \tag{12}$$

where  $P_1 = -1/2 - \kappa_{e1}$ ,  $P_2 = 1/2 - \kappa_{e1}$ ,  $P_3 = -3/2 + \kappa_{e1}$ ,  $P_4 = -1/2 - \kappa_{e2}$ ,  $P_5 = 1/2 - \kappa_{e2}$ , and  $P_6 = -3/2 + \kappa_{e2}$ . Now, combining (10)–(12), we obtain a new equation of the form:

$$\frac{\partial \psi}{\partial \tau} + A \psi \frac{\partial \psi}{\partial \xi} + \frac{\nu}{2\tau} \psi - B \frac{\partial^2 \psi}{\partial \xi^2} = 0, \tag{13}$$

where

$$A = \frac{V_p^3}{2} \left[ \frac{3}{V_p^4} - \frac{\mu_{e1} P_1 P_2 \sigma_1^2}{P_3^2} - \frac{\mu_{e2} P_4 P_5 \sigma_2^2}{P_6^2} \right], \quad (14)$$

$$B = \frac{\eta}{2}. \quad (15)$$

Equation 13 is known as MB equation modified by the extra term  $(\nu/2\tau)$  which arises due to the effect of the non-planar cylindrical ( $\nu = 1$ ) or spherical ( $\nu = 2$ ) geometry. The third term of the left-hand side of (13) represents the geometry effect while the fourth term of the left-hand side of (13) represents the dissipation effect. Equations 14 and (15) represent the nonlinear coefficient and dissipation terms, respectively.

Equation (13) shows that the term  $(\nu/2\tau)$  goes to infinity when  $\tau \rightarrow 0$ . Therefore, this term is singular at  $\tau = 0$ . For large values of  $\tau$ , this term vanishes, and we have usual Burgers equation. The governing equations are responsible for the formation and dynamics of shock waves when  $t \sim 1$ .

#### 4 Numerical Analysis

We first consider 1D planar geometry ( $\nu = 0$ ) and examine the basic features of the shock wave solutions of (13). For a frame moving with a speed  $U_0$ , the stationary shock wave solution of (13) in a planar geometry ( $\nu = 0$ ) is

$$\psi(\nu = 0) = \psi_m \left[ 1 - \tanh \left( \frac{\xi}{\Delta} \right) \right], \quad (16)$$

where  $\Delta = 2C/U_0$  is the width and  $\psi_m = U_0/A$  is the amplitude of the shock wave. It is found that for  $A > (<) 0$ , the dusty plasma supports compressive (rarefactive) DIA shock waves which are associated with a positive (negative) potential, and no shock waves exist at  $A = 0$  and  $A \sim 0$ . It is obvious that  $A$  is a function of  $\mu_{e1}$ ,  $\mu_{e2}$ ,  $\sigma_1$ ,  $\sigma_2$ ,  $\kappa_{e1}$ , and  $\kappa_{e2}$ . Therefore, to find the parametric regimes corresponding to  $A = 0$ , we have to express one (viz.  $\mu_{e1}$ ) of these six parameters in terms of the other five (viz.  $\mu_{e2}$ ,  $\sigma_1$ ,  $\sigma_2$ ,  $\kappa_{e1}$ , and  $\kappa_{e2}$ ). Therefore,  $A(\mu_{e1} = \mu_c) = 0$ , and  $\mu_c$  can be expressed as

$$\mu_{e1} = \mu_c = \frac{1}{6R_1 R_2 \sigma_1^2} [Q_1 Q_2 \sigma_1^2 - 6Q_3 Q_4 \mu_{e2} \sigma_1 \sigma_2 + \sqrt{R_1 R_2 R_3 \sigma_1^2}], \quad (17)$$

where  $Q_1 = -1 + 4\kappa_{e1}^2$ ,  $Q_2 = (3 - 2\kappa_{e2})^2$ ,  $Q_3 = 3 + 4(-2 + \kappa_{e1})\kappa_{e1}$ ,  $Q_4 = 3 + 4(-2 + \kappa_{e2})\kappa_{e2}$ ,  $R_1 = (1 - 2\kappa_{e1})^2$ ,  $R_2 = (3 - 2\kappa_{e2})^2$ ,  $R_3 = (1 + 2\kappa_{e1})^2 R_2 \sigma_1^2 - 12(-3 + 2\kappa_{e1})(1 + 2\kappa_{e1}) Q_4 \mu_{e2} \sigma_1 \sigma_2 + 12(3 - 2\kappa_{e1})^2 (-1 + 4\kappa_{e2}^2) \mu_{e2} \sigma_2^2$ .

Equation (17) represents  $\mu_c$ , the critical value of  $\mu_{e1}$  below (above), which the shock waves with a negative (positive) potential exists, gives the value of  $\mu_c$ . One can find from (17) that  $\mu_c \simeq 0.342$  for a set of dusty plasma parameters [30] (viz.  $\mu_{e2} = 0.04$ ,  $\sigma_1 = 2.5$ ,  $\sigma_2 = 0.1$ ,  $\kappa_{e1} = 20$ , and  $\kappa_{e2} = 2$ ). To find the parametric regimes for which the positive and negative potential shock profile exists, we have numerically analyzed  $A$  and obtained  $A(\mu_{e1} = \mu_c) = 0$  surface plots, hence showing shown the variation of  $\mu_c$  with  $\mu_{e2}$  and  $\sigma_1$ . The result is displayed in Fig. 1. It is clear that  $\psi_m = \infty$  at  $\mu_{e1} = \mu_c$ . This means that the small amplitude shock waves with a positive or negative potential exist for a set of dusty plasma parameters corresponding to any point which is much above or below the  $A(\mu_{e1} = \mu_c) = 0$  surfaces shown in Fig. 1. Figure 1 shows that  $\mu_c$  decreases abruptly with the increase of  $\mu_{e2}$  and increases gradually with the increase of  $\sigma_1$ . Therefore, for typical dusty plasma parameters [30] (viz.  $\sigma_1 = 1.8 - 5$ ,  $\sigma_2 = 0.1 - 0.9$ , and  $\mu_{e2} = 0.01 - 0.09$ ), we have the existence of the small amplitude shock waves with a negative or positive potential for  $\mu_{e1} < \mu_c$  or  $\mu_{e1} > \mu_c$ . However, this Burgers equation is not valid when  $\mu_{e1} \sim \mu_c$ . This is because the  $\mu_{e1} \sim \mu_c$  gives rise to infinitely large amplitude structures which break down the validity of the reductive perturbation method applied for the Burgers equation.

Since an exact analytical solution of (13) is not possible, we have numerically solved (13) and studied the effects of cylindrical ( $\nu = 1$ ) and spherical ( $\nu = 2$ ) geometries on the time-dependent DIA shock structures. We start with a large (negative) value of  $\tau$ , as for a large value of  $\tau$ , the term  $(\nu/2\tau)\psi$  is negligible. We choose in (16) this large value of  $\tau$  as our initial pulse. In Figs. 2, 3, 4, and 5, the effects of kinematic viscosity in both cylindrical and spherical geometries are investigated respectively for different values of  $\tau$ . It is found that as the magnitude of  $\tau$  increases, the shock height decreases and the effect is more pronounced in spherical geometry by comparison with the

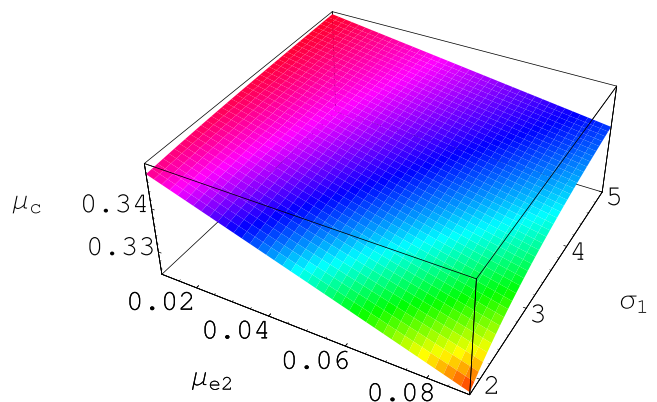


**Fig. 1** Variation of  $\mu_c$  [obtained from  $A(\mu_{e1} = \mu_c) = 0$ ] with  $\mu_{e2}$  and  $\sigma_1$  (color online)

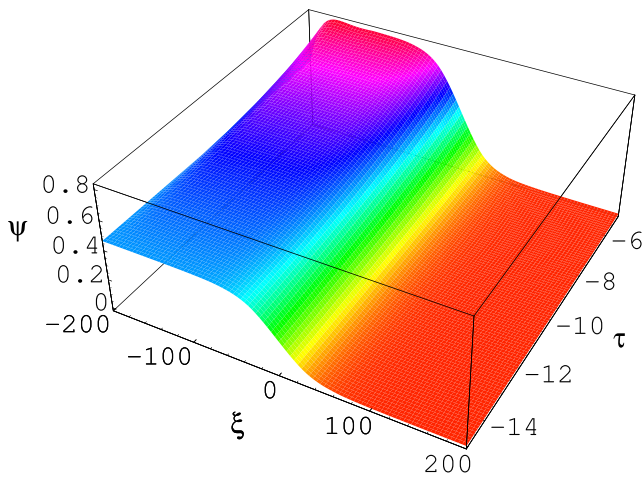


**Fig. 2** The effect of cylindrical ( $\nu = 1$ ) geometry on DIA shock structure above the critical value (for  $\mu_{e1} = 0.45$ ). Here,  $\mu_{e2} = 0.04$ ,  $\sigma_1 = 2.5$ ,  $\sigma_2 = 0.1$ ,  $\kappa_{e1} = 20$ ,  $\kappa_{e2} = 2$ , and  $U_0 = 0.1$  (color online)

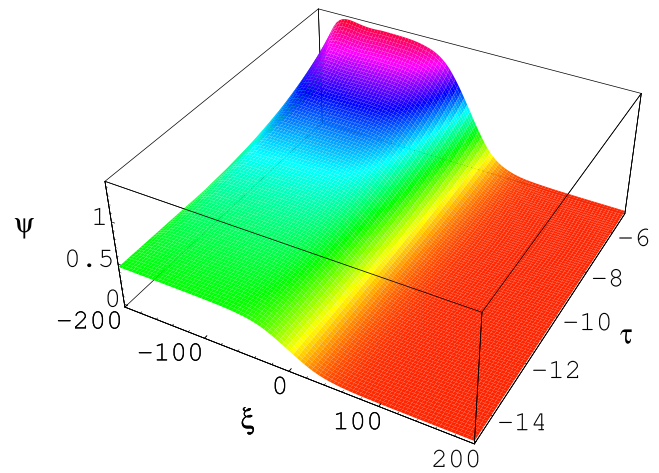


**Fig. 4** The effect of spherical ( $\nu = 2$ ) geometry on DIA shock structure above the critical value (for  $\mu_{e1} = 0.45$ ). Here,  $\mu_{e2} = 0.04$ ,  $\sigma_1 = 2.5$ ,  $\sigma_2 = 0.1$ ,  $\kappa_{e1} = 20$ ,  $\kappa_{e2} = 2$ , and  $U_0 = 0.1$  (color online)

cylindrical geometry. It is also observed that the width of the shock waves increases (decreases) with the increase of  $\eta$  ( $U_0$ ). From Fig. 9, it is seen that the spectral index parameters  $\kappa_{e1}$  and  $\kappa_{e2}$  play a significant role on the phase speed ( $V_p$ ) of DIA shock waves. The phase speed ( $V_p$ ) of DIA shock wave increases exponentially with the increase of  $\kappa_{e1}$  and decreases with the increase of  $\kappa_{e2}$ .

### 5 Discussions

We have presented a theoretical study of the propagation dynamics of cylindrical and spherical DIA shock waves in an unmagnetized dusty plasma system containing inertial ions, negatively charged static dust, and superthermal electrons with two distinct temperatures. The dynamics of the

cylindrical and spherical DIA shock wave is governed by the MB equation. Our results are summarized as follows:

1. Shock waves are formed for above and below the critical value (i.e., when  $\mu_{e1} > \mu_c$  and  $\mu_{e1} < \mu_c$ ).
2. It is observed that for  $\mu_{e1} > 0.342$ , positive (compressive) shock waves exist, whereas for  $\mu_{e1} < 0.342$ , negative (rarefactive) shock waves exist.
3. The width of the shock waves increases with the increase of  $\eta$ . It can also be said that the shock waves become smoother and weaker when the dissipation is increased. On the other hand, the width of shock waves decreases with the increase of  $U_0$ , as displayed in Fig. 6.
4. The time evolution of the cylindrical and spherical DIA shock waves significantly differs from the 1D planar DIA shock wave. It is found that as time passes, the

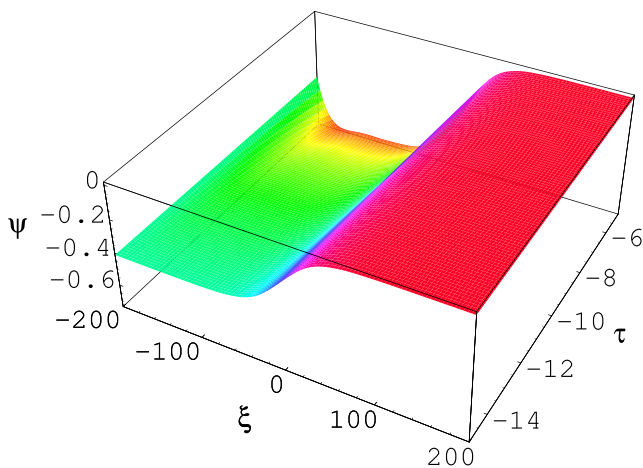


**Fig. 3** The effect of cylindrical ( $\nu = 1$ ) geometry on DIA shock structure below the critical value (for  $\mu_{e1} = 0.25$ ). Here,  $\mu_{e2} = 0.04$ ,  $\sigma_1 = 2.5$ ,  $\sigma_2 = 0.1$ ,  $\kappa_{e1} = 20$ ,  $\kappa_{e2} = 2$ , and  $U_0 = 0.1$  (color online)

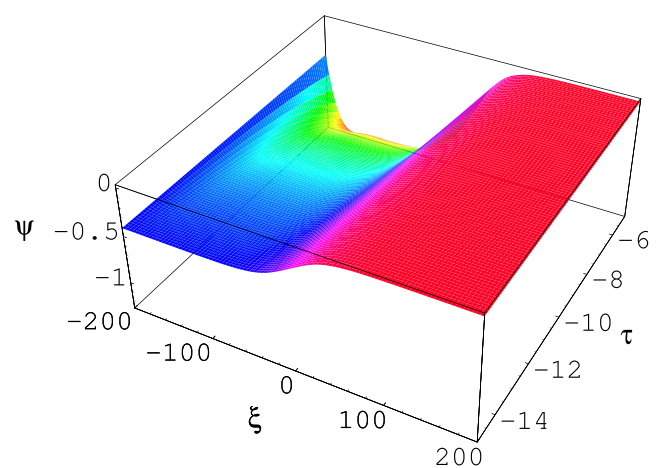


**Fig. 5** The effect of spherical ( $\nu = 2$ ) geometry on DIA shock structure below the critical value (for  $\mu_{e1} = 0.25$ ). Here,  $\mu_{e2} = 0.04$ ,  $\sigma_1 = 2.5$ ,  $\sigma_2 = 0.1$ ,  $\kappa_{e1} = 20$ ,  $\kappa_{e2} = 2$ , and  $U_0 = 0.1$  (color online)

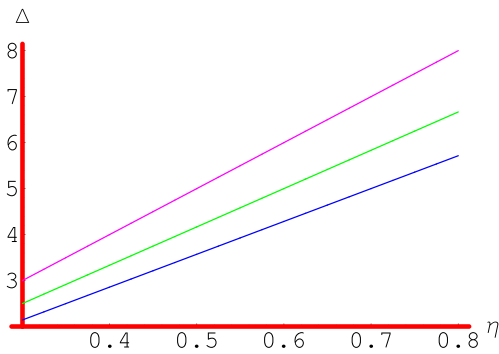


**Fig. 6** (Color online) Variation of width of shock wave with  $U_0$  and  $\eta$ . Here  $\mu_{e1} = 0.45$ ,  $\mu_{e2} = 0.04$ ,  $\sigma_1 = 2.5$ ,  $\sigma_2 = 0.1$ ,  $\kappa_{e1} = 20$ ,  $\kappa_{e2} = 2$ . The upper (pink) curve one is for  $U_0 = 0.1$ , the middle (green) one is for  $U_0 = 0.12$ , and the lower (blue) one is for  $U_0 = 0.14$

amplitude of the cylindrical and spherical DIA shocks increases.

5. The cylindrical and spherical shock waves are identical to 1D shock wave for larger value of  $\tau$  since the nonplanar geometrical effect is no longer paramount for larger value of  $\tau$ . However, as the value of  $\tau$  decreases, the nonplanar geometrical effect, represented by  $\frac{v\psi}{2\tau}$ , will become dominant and the cylindrical, spherical, and 1D shock waves differ from each other.
6. Figures 7 and 8 indicate the dependency of the amplitude of DIA shocks to the superthermality effects. They show that the spectral index parameters ( $\kappa_{e1}$  and  $\kappa_{e2}$ ) have a strong effect on the wave behavior. It is found that the amplitude of DIA shocks increases when the spectral index parameter  $\kappa_{e2}$  increases (displayed in Fig. 7). With the increasing of spectral index parameter  $\kappa_{e1}$ , the amplitude of DIA shocks decreases (displayed in Fig. 8).
7. The height and steepness of cylindrical shock wave are larger than that of the 1D shock wave but smaller than that of the spherical shock wave. In other words, the amplitude of the cylindrical DIA shock wave is larger

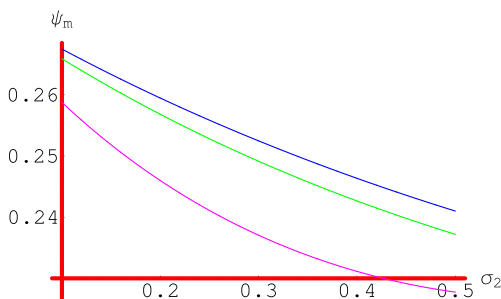


**Fig. 7** The variation of amplitude of the positive shock profiles with  $\kappa_{e2}$  and  $\sigma_2$ . Here  $\mu_{e1} = 0.45$ ,  $\mu_{e2} = 0.04$ ,  $\sigma_1 = 2.5$ ,  $\eta = 0.3$ ,  $\kappa_{e1} = 20$ , and  $U_0 = 0.1$ . The upper (blue) curve is for  $\kappa_{e2} = 4$ , the middle (green) one is for  $\kappa_{e2} = 3$ , and the lower (pink) one is for  $\kappa_{e2} = 2$  (color online)

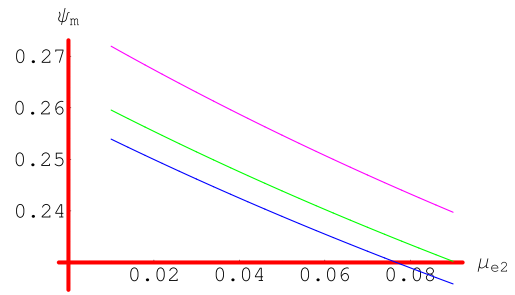


**Fig. 8** The variation of amplitude of the positive shock profiles with  $\kappa_{e1}$  and  $\mu_{e2}$ . Here,  $\mu_{e1} = 0.45$ ,  $\sigma_1 = 2.5$ ,  $\sigma_2 = 0.1$ ,  $\eta = 0.3$ ,  $\kappa_{e2} = 2$ , and  $U_0 = 0.1$ . The upper (pink) curve is for  $\kappa_{e1} = 20$ , the middle (green) one is for  $\kappa_{e1} = 30$ , and the lower (blue) one is for  $\kappa_{e1} = 40$  (color online)

than that of the 1D planar DIA shock, but smaller than that of the spherical DIA shock wave. Furthermore, the spherical DIA shock waves move faster as compared to the corresponding cylindrical DIA shock waves.

8. The variation of the phase speed ( $V_p$ ) with the spectral index parameters  $\kappa_{e1}$  and  $\kappa_{e2}$  is explored in Fig. 9. It is observed that the phase speed ( $V_p$ ) increases exponentially with the increase of the spectral index parameter  $\kappa_{e1}$  and decreases with the increase of  $\kappa_{e2}$ . Therefore, it can be said that electron superthermality parameters ( $\kappa_{e1}$  and  $\kappa_{e2}$ ) play an important role on the phase speed of DIA shock waves.

The nonplanar geometry effect for DIA shock wave is very strong for a small value of  $\tau$ , and there are obvious differences between the cylindrical and spherical DIA shock waves regarding both amplitudes and widths of the structures. It is seen that the amplitude increases with increase in  $\tau$  as well as the value of superthermal or spectral index parameter  $\kappa_{e2}$  and the amplitude decreases with the increase of spectral index parameter  $\kappa_{e1}$ . Besides, a small value of spectral index parameter and thus an increase in superthermality increases the speed of DIA shock waves. Thus, spectral index parameters  $\kappa_{e1}$  and  $\kappa_{e2}$  have a significant

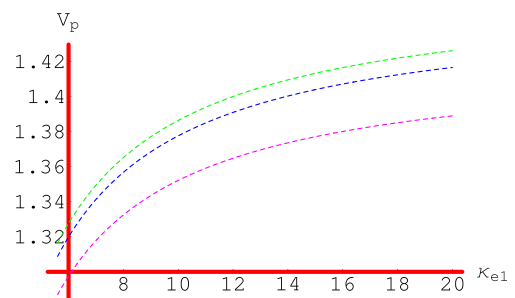


**Fig. 9** The variation of phase velocity with  $\kappa_{e1}$  and  $\kappa_{e2}$  above the critical value (for  $\mu_{e1} = 0.45$ ). Here,  $\sigma_1 = 1$ ,  $\sigma_2 = 0.1$ , and  $\mu_{e2} = 0.04$ . The upper (green) curve is for  $\kappa_{e2} = 1.6$ , the middle (blue) one is for  $\kappa_{e2} = 1.8$ , and the lower (pink) one is for  $\kappa_{e2} = 2$  (color online)

influence on the formation of shock structures in our present plasma model. It may be noted that because of electron superthermality and also other plasma parameters (viz.  $\sigma_1$ ,  $\sigma_2$ ,  $\mu_{e1}$ ,  $\mu_{e2}$ , etc.), the DIA shock wave may exhibit either a compression or a rarefaction.

We hope that our theoretical present work based on nonplanar geometry should be useful for understanding the electrostatic disturbances in most laboratory devices [such as capsule implosion (spherical geometry), shock tube (cylindrical geometry), etc.] which are of spherical or cylindrical shape. This theoretical work can also be applied in some space plasma systems (viz. magnetosphere, pulsar magnetosphere [41], Saturn's outer magnetosphere ( $R \sim 13-18 R_S$ , where  $R_S$  is the radius of Saturn) [26], Saturn's inner magnetosphere [26] ( $R < 9 R_S$ , etc.) which are also of spherical shape. We finally add that stability analysis of these shock structures, investigation of the features of arbitrary amplitude shock structures, and the effect of external magnetic field on the properties of these shock structures are also problems of great importance, but beyond the scope of our present work.

## References

- N. D'Angelo, Planet. Space Sci. **38**, 1143 (1990)
- P.K. Shukla, V.P. Silin, Phys. Scr. **45**, 508 (1992)
- A. Barkan, N. D'Angelo, R.L. Merlino, Planet. Space Sci. **44**, 239 (1996)
- Y. Nakamura, H. Bailung, P.K. Shukla, Phys. Rev. Lett. **83**, 1602 (1999)
- M.M. Rahman, M.S. Alam, A.A. Mamun, J. Korean Phys. Soc. **64**, 1828 (2014)
- Y. Nakamura, Phys. Plasmas **9**, 440 (2002)
- Q.Z. Luo, N. D'Angelo, R.L. Merlino, Phys. Plasmas **7**, 3457 (1999)
- A.A. Mamun, P.K. Shukla, IEEE Trans. Plasma Sci. **30**, 720 (2002)
- B. Eliasson, P.K. Shukla, Phys. Plasmas **12**, 024502 (2005)
- S. Sultana, G. Sarri, I. Kourakis, Phys. Plasmas **19**, 012310 (2012)
- H. Abbasi, H.H. Pajouth, Phys. Plasmas **12**, 024502 (2005)
- N.S. Saini, I. Kourakis, M.A. Hellberg, Phys. Plasmas **16**, 062903 (2009)
- V.M. Vasyliunas, J. Geophys. Res. **73**, 2839 (1968)
- M.P. Leubner, J. Geophys. Res. **87**, 6335 (1982)
- D. Summers, R.M. Thorne, Phys. Fluids B **3**, 1835 (1991)
- R.L. Mace, M.A. Hellberg, Phys. Plasmas **2**, 2098 (1995)
- T.K. Baluku, M.A. Hellberg, Phys. Plasmas **15**, 123705 (2008)
- M.A. Hellberg, R.L. Mace, T.K. Baluku, I. Kourakis, N.S. Saini, Phys. Plasmas **16**, 094701 (2009)
- T.K. Baluku, M.A. Hellberg, I. Kourakis, N.S. Saini, Phys. Plasmas **17**, 053702 (2010)
- T.K. Baluku, M.A. Hellberg, Phys. Plasmas **19**, 012106 (2012)
- M.S. Alam, M.J. Uddin, M.M. Masud, A.A. Mamun, Chaos **24**, 033130 (2014)
- H. Alinejad, M. Tribeche, M.A. Mohammadi, Phys. Lett. A **375**, 4183 (2011)
- M. Shahmansouri, H. Alinejad, Astrophys. Space Sci. **343**, 257 (2013)
- M.S. Alam, M.M. Masud, A.A. Mamun, Chin. Phys. B **22**, 115202 (2013)
- P. Schippers, M. Blanc, N. André, I. Dandouras, G.R. Lewis, L.K. Gilbert, A.M. Persoon, N. Krupp, D.A. Gurnett, A.J. Coates, S.M. Krimigis, D.T. Young, M.K. Dougherty, J. Geophys. Res. **113**, A07208 (2008)
- T.K. Baluku, M.A. Hellberg, R.L. Mace, J. Geophys. Res. **116**, A04227 (2011)
- M.S. Alam, M.M. Masud, A.A. Mamun, Plasma Phys. Rep. **39**, 1011 (2013)
- M.S. Alam, *Dust-ion-acoustic waves in dusty plasmas with superthermal electrons* (LAP LAMBERT Academic Publishing, Germany, 2013). ISBN-10: 3659509523
- M. Shahmansouri, B. Shahmansouri, D. Darabi, Indian J. Phys. **87**, 711 (2013)
- M.S. Alam, M.M. Masud, A.A. Mamun, Astrophys. Space Sci. **349**, 245 (2014)
- S. Sultana, A.A. Mamun, Astrophys. Space Sci. **349**, 229 (2014)
- S. Sultana, S. Islam, A.A. Mamun, Astrophys. Space Sci. **351**, 581 (2014)
- M.M. Rahman, M.S. Alam, A.A. Mamun, Astrophys. Space Sci. **352**, 193 (2014)
- J.-K. Xue, Phys. Plasmas **10**, 4893 (2003)
- A.A. Mamun, P.K. Shukla, Euro. Phys. Lett. **87**, 25001 (2009)
- B. Sahu, M. Tribeche, Phys. Plasmas **19**, 022304 (2012)
- S. Yasmin, M. Asaduzzaman, A.A. Mamun, J. Plasma Phys. **79**, 545 (2013)
- D.K. Ghosh, P. Chatterjee, P.K. Mandal, B. Sahu, Pramana **81**, 491 (2013)
- A.A. Mamun, R.A. Cairns, Phys. Rev. E **79**, 055401 (2009)
- P.K. Shukla, A.A. Mamun, *Introduction to Dusty Plasma Physics*. CRC Press (2010)
- S.K. Kundu, D.K. Ghosh, P. Chatterjee, B. Das, Bulg. J. Phys. **38**, 409 (2011)